

# Near-infrared linewidth narrowing in plasmonic Fano-resonant metamaterials via tuning of multipole contributions

Wen Xiang Lim, , Song Han, , Manoj Gupta, , Kevin F. MacDonald, and , and Ranjan Singh

Citation: *Appl. Phys. Lett.* **111**, 061104 (2017); doi: 10.1063/1.4997423

View online: <http://dx.doi.org/10.1063/1.4997423>

View Table of Contents: <http://aip.scitation.org/toc/apl/111/6>

Published by the [American Institute of Physics](#)

---

## Articles you may be interested in

[Active tuning of high-Q dielectric metasurfaces](#)

*Applied Physics Letters* **111**, 053102 (2017); 10.1063/1.4997301

[Optically active dilute-antimonide III-nitride nanostructures for optoelectronic devices](#)

*Applied Physics Letters* **111**, 061101 (2017); 10.1063/1.4997450

[A three-dimensional all-metal terahertz metamaterial perfect absorber](#)

*Applied Physics Letters* **111**, 051101 (2017); 10.1063/1.4996897

[Broadband acoustic energy confinement in hierarchical sonic crystals composed of rotated square inclusions](#)

*Applied Physics Letters* **111**, 054103 (2017); 10.1063/1.4985230

[Terahertz polarization mode conversion in compound metasurface](#)

*Applied Physics Letters* **111**, 031107 (2017); 10.1063/1.4994156

[Wannier Koopman method calculations of the band gaps of alkali halides](#)

*Applied Physics Letters* **111**, 054101 (2017); 10.1063/1.4996743

---



## Near-infrared linewidth narrowing in plasmonic Fano-resonant metamaterials via tuning of multipole contributions

Wen Xiang Lim,<sup>1,2,3</sup> Song Han,<sup>1,2</sup> Manoj Gupta,<sup>1,2</sup> Kevin F. MacDonald,<sup>3</sup> and Ranjan Singh<sup>1,2,a)</sup>

<sup>1</sup>*Division of Physics and Applied Physics, School of Physical and Mathematical Sciences, Nanyang Technological University, Singapore 637371, Singapore*

<sup>2</sup>*Centre for Disruptive Photonic Technologies, The Photonics Institute, Nanyang Technological University, 50 Nanyang Avenue, Singapore 639798, Singapore*

<sup>3</sup>*Optoelectronics Research Centre and Centre for Photonic Metamaterials, University of Southampton, Southampton SO17 1BJ, United Kingdom*

(Received 19 May 2017; accepted 24 July 2017; published online 8 August 2017)

We report on an experimental and computational (multipole decomposition) study of Fano resonance modes in complementary near-IR plasmonic metamaterials. Resonance wavelengths and linewidths can be controlled by changing the symmetry of the unit cell so as to manipulate the balance among multipole contributions. In the present case, geometrically inverting one half of a four-slot (paired asymmetric double bar) unit cell design changes the relative magnitude of magnetic quadrupole and toroidal dipole contributions leading to the enhanced quality factor, figure of merit, and spectral tuning of the plasmonic Fano resonance. *Published by AIP Publishing.*

[<http://dx.doi.org/10.1063/1.4997423>]

Metamaterials have been a subject of intense interest due to their ability to exhibit optical properties not commonly found in natural materials. By suitably engineering the size and geometry of metamaterials at the sub-wavelength scale, researchers have been able to exploit and manipulate electromagnetic waves to achieve various phenomena such as invisibility cloaking,<sup>1-4</sup> super lenses,<sup>5-8</sup> electromagnetically induced transparency,<sup>9-11</sup> and high quality-factor Fano resonances,<sup>12-15</sup> offering a rich variety of applications in photonics and optics. Specifically, a Fano resonance is a scattering phenomenon resulting from destructive interference between a continuum background and a resonant mode and is commonly recognized by its asymmetric lineshape. In 1935, Fano was the first to theoretically formulate an equation which adequately provides an explanation of this unique and distinct lineshape.<sup>16</sup> In the field of plasmonic metamaterials, various Fano resonant unit cell shapes and designs such as dolmen structures,<sup>17-19</sup> ring/disk nanocavities,<sup>20-23</sup> heptamers,<sup>24-28</sup> and notably split ring resonators<sup>29-33</sup> have been explored in great detail. An uncomplicated design composed of paired asymmetric double bars (ADBs) has also been studied for its Fano resonance<sup>34-39</sup> and electromagnetically induced transparency properties.<sup>40-43</sup> While computed charge distribution and field vectors are typically used as a visual mechanism to identify and attribute the origin of the Fano resonance in such structures, there has been little focus on quantitative and qualitative analysis of the role of the multipoles that contribute to the asymmetric line shape and the linewidth narrowing of Fano resonances in complementary nanostructures (paired asymmetric double slots in a thin plasmonic metal film). Complementary nanostructures are interesting due to the enhanced mode volume as a result of the tight confinement of the electromagnetic fields in the narrow empty spaces of the nanostructures (portions without metal). Since the mode

volume is higher in these nanostructures, the interaction of the Fano cavity with any other dynamic material medium would be extremely strong. As such, the multipole expansion analysis is applied to this simple design as an illustration of the way in which it can enrich the understanding of symmetry-broken metamaterials in complementary designs.

Here, we introduce a comparison between complementary nanostructures of paired ADBs in so-called “Fano” and “iFano” configurations (iFano denoting a 180° inversion of one ADB relative to the Fano geometry—as shown in Fig. 1) and report that in the iFano configuration, a larger figure of merit and quality factor can be achieved in the infrared regime, as compared to the Fano configuration. Numerical simulations attribute the origin of a broad dipolar resonance to the electric dipole, and the asymmetric Fano lineshape is a consequence of the electric dipole (E. dip) interacting with the magnetic quadrupole (M. quad) and the toroidal dipole (T. dip). Via a decomposition of the multipoles, we find that the magnetic quadrupole competes on the same scale as the toroidal dipole to narrow the linewidth of the resonance. In addition, the iFano configuration offers a spectral shift without the need to alter the periodicity or dimensions of the unit cell.

Figure 1(a) illustrates a generic unit cell of the metamaterial nanostructure used in the present study, which comprises four slots (two complementary ADBs) in a thin gold film. In the “Fano” configuration, the ADBs have the same orientation, while in the iFano configuration one ADB is rotated by 180° with respect to the other. The period of the unit cell is fixed at  $p_x = 1400$  nm and  $p_y = 700$  nm, the long bar length is fixed at  $l = 420$  nm, and the  $x$ -separation between ADBs within the unit cell is fixed at  $g = 80$  nm. Within the double bars, the long and short bars are separated by a distance  $d = 140$  nm. The asymmetry of the nanostructures was controlled by varying the lengths of the short bar, from 420 nm to 100 nm. The asymmetry parameter is defined as the ratio of

<sup>a)</sup>Email: ranjans@ntu.edu.sg

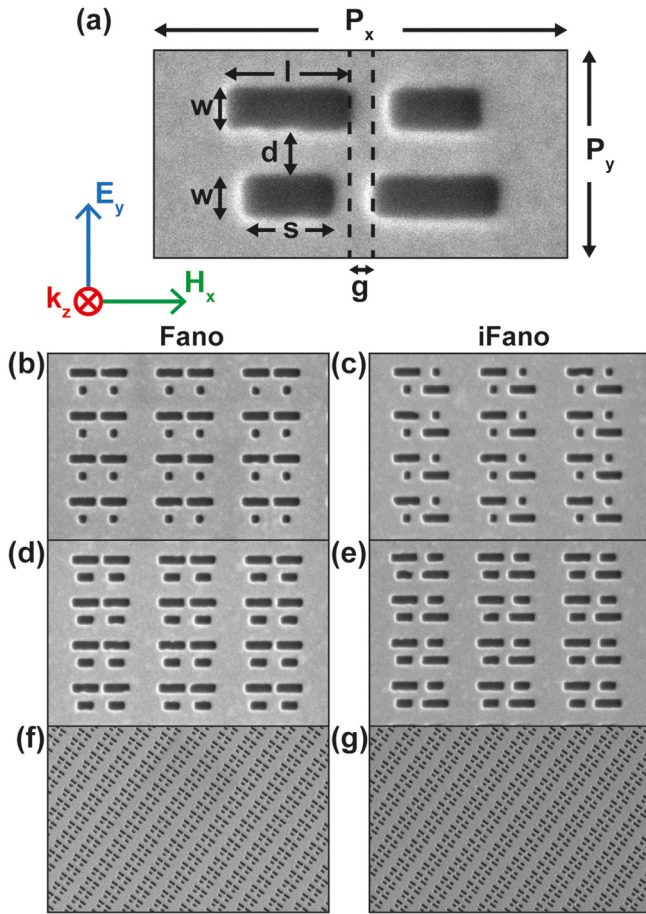


FIG. 1. (a) Dimensions of a single unit cell of paired ADBs in the iFano configuration. In experiment and numerical simulation, light is normally incident on the plane of the nanostructure with the electric field polarized along the  $y$ -axis and magnetic field in the  $x$ -axis. Scanning electron microscope (SEM) images of the complementary nanostructures in Fano (b, d) and iFano (c, e) configurations with asymmetry parameters of 0.762 (b, c) and 0.286 (d, e). A perspective view of Fano (f) and iFano (g) configurations at an oblique viewing angle of  $52^\circ$  is shown.

the difference between the length of the long ( $l$ ) and short ( $s$ ) bars and the length of the long bar,  $\alpha = \frac{l-s}{l}$ . Figures 1(b)–1(e) show scanning electron microscopy (SEM) images of fabricated complementary Fano and corresponding iFano configurations for asymmetry parameters of 0.762 and 0.289, respectively. Experimental samples were fabricated in a 40 nm gold thin film evaporated onto a quartz substrate at a rate of  $0.2 \text{ \AA/s}$ . Each array of complementary nanostructures has the dimensions of  $40 \mu\text{m} \times 40 \mu\text{m}$  and is fabricated by focused-ion beam milling (FEI Helios Nanolab 650 DualBeam operating at 30 kV and 24 pA). The reflectance spectra of fabricated nanostructures were measured using a microspectrophotometer (Jasco MSV-5200) with  $y$ -polarized incident light. Numerical simulations were carried out using commercial finite-difference time-domain Maxwell solver software (Lumerical FDTD) assuming plane wave illumination polarized in the  $y$ -direction. Periodic boundary conditions were imposed in the  $x$ - and  $y$ -directions; perfectly matched layers were set in the  $z$ -direction so that any incident waves do not reflect at the boundaries but are strongly absorbed. The optical constants of gold were taken from Johnson and Christy,<sup>44</sup> and the refractive index of the quartz substrate was set to 1.5.

Figures 2(a) and 2(b) show the reflectance spectra measured for  $y$ -polarized incident light propagating normal to the plane of the nanostructures. They clearly illustrate that in both configurations, the Fano resonance red-shifts with decreasing asymmetry accompanied by linewidth narrowing. For a pair of *symmetric* double bars in both configurations, the resonance broadens and resembles a simple dipole resonance at around 1300 nm. In contrast, for non-zero asymmetry parameters, the broad dipolar resonance evolves into a Fano resonance centred at around 1400 nm for the iFano configuration at the highest level of asymmetry ( $\alpha = 0.762$ ) - a wavelength that is markedly shorter than the resonance wavelength of the Fano configuration, at around 1600 nm. Numerically simulated reflectance spectra, shown in Figs. 2(c) and 2(d), are in excellent agreement with the experimentally observed optical response, with the slight discrepancies in resonance wavelengths being attributed to imperfections incurred during the fabrication process (i.e., deviations from the ideal rectilinear geometry assumed in modelling) and differences in the optical constants of materials used in the simulations. It is evident from Figs. 2(e) and 2(f) that for a given value of the asymmetry parameter, the linewidth of the iFano configuration is narrower than the Fano configuration. The blue-shift of the entire spectrum from the Fano configuration to iFano configuration is a result of a decrease in the electromagnetic coupling between the in-plane modes of the long bars in the latter case.<sup>45</sup>

Quality factors of the plasmonic system were evaluated for both configurations at their respective resonances. The quality ( $Q$ ) factor is a dimensionless parameter which determines the extent of radiative and non-radiative losses in the plasmonic resonator. It is calculated here as a ratio between the resonance wavelength,  $\lambda_0$  and the full-width at half maximum,  $\delta\lambda$  of the resonance dip in the reflectance spectra,  $Q = \frac{\lambda_0}{\delta\lambda}$ . A plasmonic system is less damped when the  $Q$ -factor is higher, and the system can store more energy. As shown in Fig. 3, measured and simulated  $Q$ -factors for the Fano configuration increase with decreasing asymmetry to values of 34.9 and 45.7, respectively, at  $\alpha = 0.048$ . From simulations, the  $Q$ -factor of the iFano configuration reaches 75.4 at  $\alpha = 0.048$ , a value more than 1.5 times (50%) larger than the corresponding Fano configuration. However, at these small values of the asymmetry parameter, experimental  $Q$ -factors cannot be evaluated due to the weakness of the resonance, which appears as a shoulder as opposed to a defined dip in the reflectance spectrum [Fig. 2(b)]. Another parameter which characterises the overall performance of the Fano resonance is the figure of merit (FoM), defined as the product of the  $Q$ -factor and the peak-to-peak resonant intensity. The FoM parameter is crucial as it considers the trade-off between the quality factor and the intensity of the Fano resonance. Typically, the  $Q$  factor of a Fano resonant system decreases as the resonance intensity increases when the asymmetry in the system is increased. From Fig. 3, the measured and simulated FoM in both configurations suggest that the system has optimum performance near  $\alpha = 0.4$  and 0.3, respectively. We observe reasonable agreement between the measured and simulated trends in both the  $Q$ -factor and FoM of the Fano and iFano configurations.

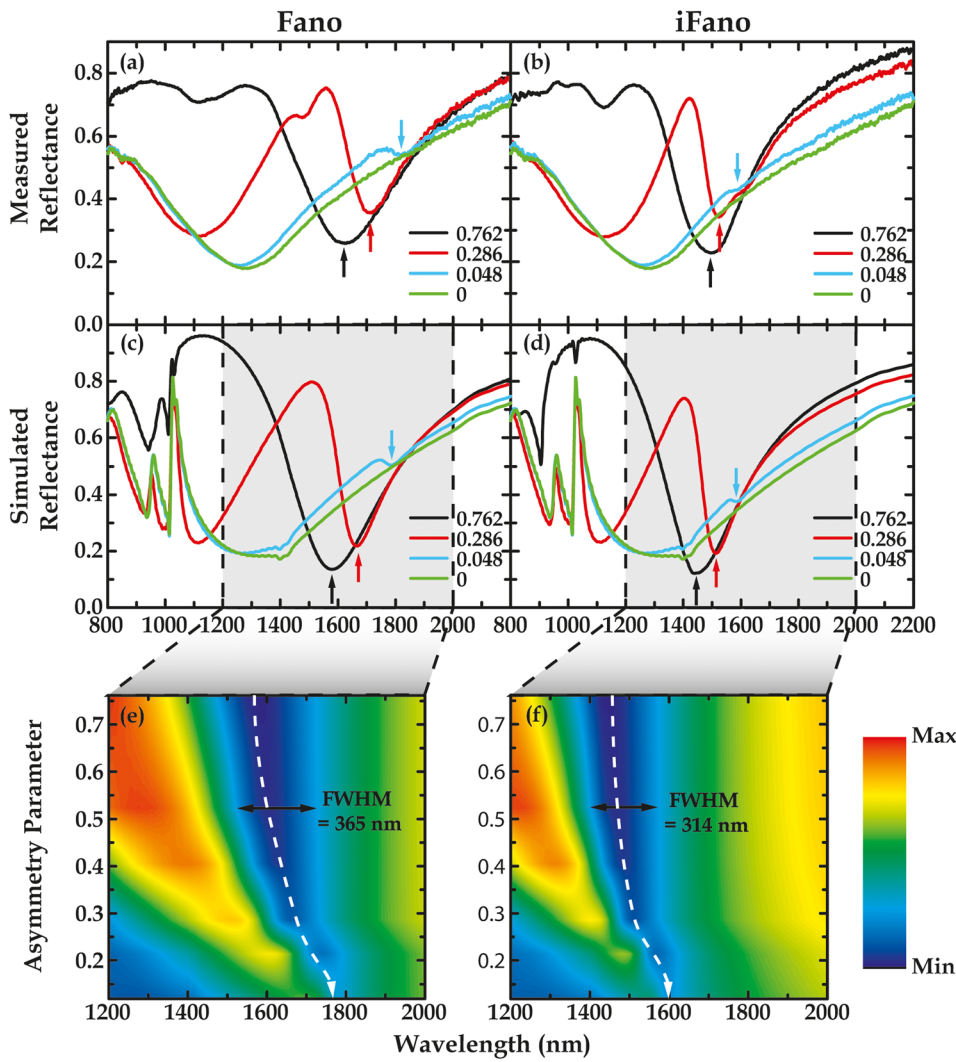


FIG. 2. Measured (a, b) and simulated (c, d) reflectance spectra of the complementary Fano (a, c) and iFano (b, d) configurations for a selection of asymmetry parameters. The dips of the Fano resonances are marked with arrows in the corresponding line colour. Colour maps of simulated reflectance against wavelength and asymmetry parameter for the (e) Fano and (f) iFano configuration. In these figures, the black arrow highlights, by way of example, the linewidth of the Fano resonance for  $\alpha = 0.524$ . The white dashed line illustrates the tuning extent of resonance wavelength over the range of asymmetry parameters considered.

To better understand the nature of the optical responses in different configurations and its influence on the linewidth narrowing, numerical calculations were performed using a multipole expansion of the electromagnetic fields. The

calculated induced current densities in the nanostructures were used to compute the scattering power of several multipoles, which can be represented in the  $x, y, z$  Cartesian coordinate frame as follows:<sup>46–48</sup>

$$\text{Electric dipole moment: } P_\alpha = \frac{1}{i\omega} \int J_\alpha d^3r,$$

$$\text{Magnetic dipole moment: } M_\alpha = \frac{1}{2c} \int (\mathbf{r} \times \mathbf{J})_\alpha d^3r,$$

$$\text{Toroidal dipole moment: } T_\alpha = \frac{1}{10c} \int [(\mathbf{r} \cdot \mathbf{J})r_\alpha - 2r^2 J_\alpha] d^3r,$$

$$\text{Electric quadrupole moment: } Q_{\alpha\beta} = \frac{1}{i2\omega} \int \left[ r_\alpha J_\beta + r_\beta J_\alpha - \frac{2}{3} (\mathbf{r} \cdot \mathbf{J}) \delta_{\alpha\beta} \right] d^3r,$$

$$\text{Magnetic quadrupole moment: } M_{\alpha\beta} = \frac{1}{3c} \int [(\mathbf{r} \times \mathbf{J})_\alpha r_\beta + (\mathbf{r} \times \mathbf{J})_\beta r_\alpha] d^3r,$$

where  $c$  is the speed of light,  $J$  is the induced current density, and  $\alpha, \beta = x, y, z$ .

In both configurations, this analysis reveals that the appearance of the broad resonance for paired symmetric double bars can be attributed to an electric dipole which

oscillates in phase with incident electromagnetic waves. As the length of the short bar starts to decrease, the symmetry of the nanostructures is broken, resulting in the excitation of the Fano resonance. In the asymmetric case, crucial higher-order contributions come from the toroidal dipole and magnetic

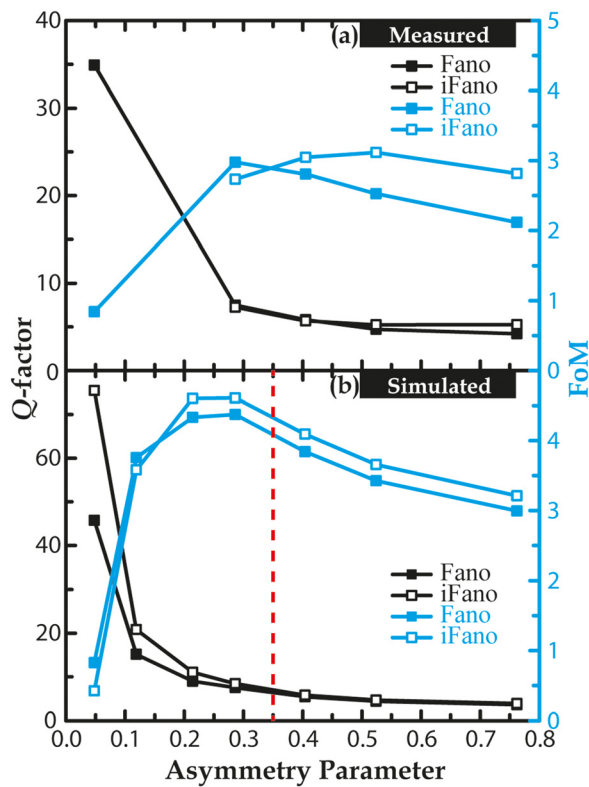


FIG. 3. (a) Measured and (b) simulated  $Q$ -factor and FoM of the complementary Fano and iFano configurations as functions of asymmetry parameter.

quadrupole alongside the fundamental electric dipole as illustrated in Fig. 4 (magnetic dipole and electric quadrupole contributions by comparison are negligible). In general, the electric dipole is highly radiative and couples easily with the driving field. Although the electric dipole plays a determinative role in the appearance of the Fano resonance, the higher-order contributions of the toroidal dipole and the magnetic quadrupole cannot be neglected. As the asymmetry between the double bars is introduced in both configurations, there is an increase in their contributions and together they interact

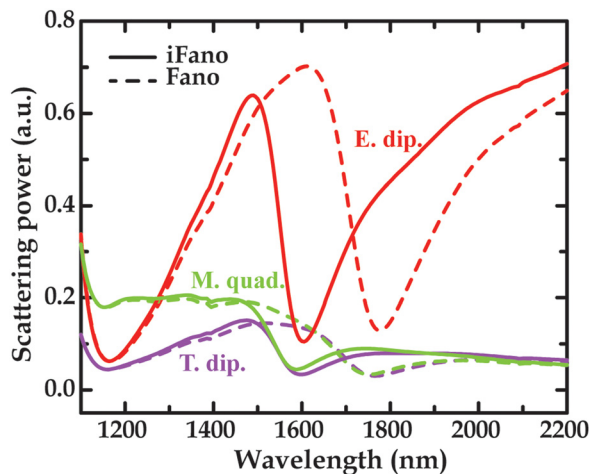


FIG. 4. The scattering power of the major contributing multipoles evaluated from the induced current densities of a unit cell in Fano (dotted lines) and iFano (solid lines) configurations for an asymmetry parameter of 0.289. The magnetic dipole and electric quadrupole contributions are negligible and therefore not shown.

with the electric dipole to form an asymmetric Fano resonance. The consequence is the narrowing of the linewidth of the resonance wavelength and a higher  $Q$ -factor obtained as compared to the symmetric system.

A closer look at the total contributions of the scattering power by the multipoles at resonance reveals that the sum of the scattering power due to the electric dipole, magnetic quadrupole, and toroidal dipole in the Fano configuration is greater than that in the iFano configuration, as shown in Fig. 5(a). This accounts for the higher  $Q$ -factor observed for the iFano configuration as compared to the Fano configuration. To understand the individual roles of the toroidal dipole and magnetic quadrupole, we evaluated the difference between their scattering powers and found that for all values of the asymmetry parameters, there is a larger difference in the iFano configuration as compared to the Fano configuration. In both configurations, as shown in Fig. 5(b), below an asymmetry parameter of  $\alpha = 0.35$ , the difference between the scattering powers of the toroidal dipole and magnetic quadrupole starts to diverge. This corresponds to the point at which the  $Q$ -factor in Fig. 3(b) increases more rapidly with the decreasing asymmetry parameter in the iFano configuration as compared to the Fano configuration. This indicates that the response of the magnetic quadrupole dominates the toroidal dipole in the iFano configuration. In the Fano configuration, the toroidal dipole slowly suppresses the response of the magnetic quadrupole and the difference starts to reduce. As a result, we can conclude that with regards to the linewidth narrowing of the Fano resonance, the magnetic

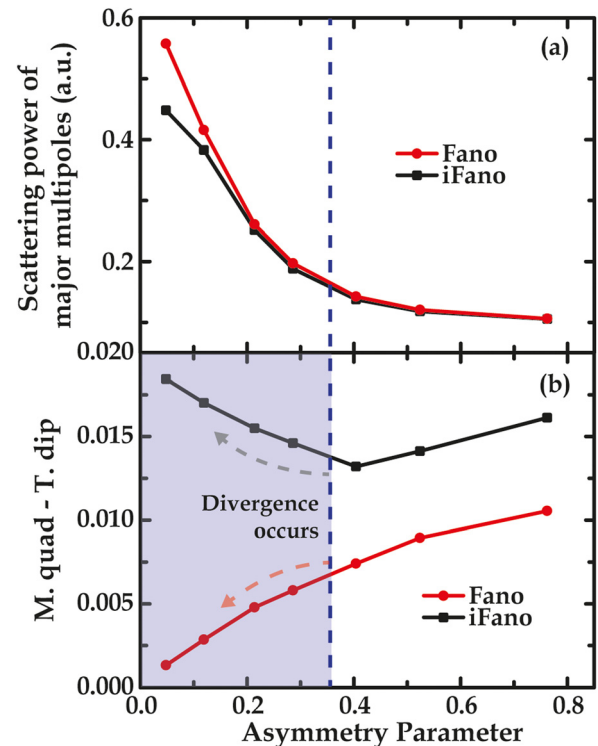


FIG. 5. (a) The sum of the scattering powers of the major contributing multipoles evaluated from the induced current densities of a unit cell in the metamaterial and (b) The difference between scattering powers of the magnetic quadrupole and the toroidal dipole, as functions of asymmetry parameter for the Fano and iFano configurations.

quadrupole plays a significant role in the resonant line narrowing while the toroidal dipole competes with the magnetic quadrupole to broaden the resonance in the complementary paired ADBs system. With the iFano configuration, we can increase the dominance of the magnetic quadrupole and narrow the linewidth to improve the  $Q$ -factor. Moreover, by simply inverting one ADB in the paired ADB unit cell, it is possible to blue-shift the near-infrared resonance by as much as 200 nm ( $\sim 12.5\%$ ), providing for facile spectral tuning without a change of structural dimensions.

In conclusion, multipolar decomposition provides an informative and broadly applicable approach to the analysis of resonant modes in complementary plasmonic metamaterial structures. For the complementary paired ADB metamaterial arrays presented in this work, such analysis demonstrates that the optical response of the nanostructures is mainly due to interactions between the electric dipole, magnetic quadrupole, and the toroidal dipole. The plasmonic systems in “Fano” and “iFano” configurations (“i” denoting the geometric inversion of part of the unit cell) are similar but for an iFano configuration, the contribution of the magnetic quadrupole is enhanced relative to the toroidal dipole, which results in the linewidth narrowing of the Fano resonance. The achievable  $Q$ -factor in the iFano configuration is enhanced by as much as 1.5 times compared to the Fano configuration. Aside from enhancing the  $Q$ -factor, it is notable here that the inverted configuration also provides a mechanism to widen the tunability in the infrared spectral range without a need to change the shape or dimensions of the metamaterial unit cell—a behaviour that may be of particular use in optical and bio-sensing applications.

This work was supported by research grants from Nanyang Technological University Start-up Grant No. M4081282, Singapore Ministry of Education Grant Nos. MOE2011-T3-1-005 and MOE2015-T2-2-103, and the Engineering and Physical Sciences Research Council, UK Grant No. EP/M009122/1.

Following a period of embargo, the data from this paper will be available from the University of Southampton research repository at <http://doi.org/10.5258/SOTON/D0158>.

- <sup>1</sup>D. Schurig, J. J. Mock, B. J. Justice, S. A. Cummer, J. B. Pendry, A. F. Starr, and D. R. Smith, *Science* **314**, 977 (2006).
- <sup>2</sup>J. B. Pendry, D. Schurig, and D. R. Smith, *Science* **312**, 1780 (2006).
- <sup>3</sup>H. Y. Chen, C. T. Chan, and P. Sheng, *Nat. Mater.* **9**, 387 (2010).
- <sup>4</sup>T. Ergin, N. Stenger, P. Brenner, J. B. Pendry, and M. Wegener, *Science* **328**, 337 (2010).
- <sup>5</sup>N. Fang, H. Lee, C. Sun, and X. Zhang, *Science* **308**, 534 (2005).
- <sup>6</sup>X. Zhang and Z. Liu, *Nat. Mater.* **7**, 435 (2008).
- <sup>7</sup>N. Fang, D. Xi, J. Xu, M. Ambati, W. Srituravanich, C. Sun, and X. Zhang, *Nat. Mater.* **5**, 452 (2006).
- <sup>8</sup>V. M. Shalaev, *Nat. Photonics* **1**, 41 (2007).
- <sup>9</sup>S. Zhang, D. A. Genov, Y. Wang, M. Liu, and X. Zhang, *Phys. Rev. Lett.* **101**, 047401 (2008).
- <sup>10</sup>J. Gu, R. Singh, X. Liu, X. Zhang, Y. Ma, S. Zhang, S. A. Maier, Z. Tian, A. K. Azad, H. T. Chen, A. J. Taylor, J. Han, and W. Zhang, *Nat. Commun.* **3**, 1151 (2012).
- <sup>11</sup>N. Papisimakis, V. A. Fedotov, N. I. Zheludev, and S. L. Prosvirnin, *Phys. Rev. Lett.* **101**, 253903 (2008).

- <sup>12</sup>B. Luk'yanchuk, N. I. Zheludev, S. A. Maier, N. J. Halas, P. Nordlander, H. Giessen, and C. T. Chong, *Nat. Mater.* **9**, 707 (2010).
- <sup>13</sup>V. A. Fedotov, M. Rose, S. L. Prosvirnin, N. Papisimakis, and N. I. Zheludev, *Phys. Rev. Lett.* **99**, 147401 (2007).
- <sup>14</sup>R. Singh, I. Al-Naib, W. Cao, C. Rockstuhl, M. Koch, and W. Zhang, *IEEE Trans. Terahertz Sci. Technol.* **3**(6), 820 (2013).
- <sup>15</sup>M. Rahmani, B. Luk'yanchuk, and M. Hong, *Laser Photonics Rev.* **7**, 329 (2013).
- <sup>16</sup>U. Fano, *Phys. Rev.* **124**, 1866 (1961).
- <sup>17</sup>N. Verellen, Y. Sonnefraud, H. Sobhani, F. Hao, V. V. Moshchalkov, P. V. Dorpe, P. Nordlander, and S. A. Maier, *Nano Lett.* **9**, 1663–1667 (2009).
- <sup>18</sup>B. Gallinet and O. J. F. Martin, *Phys. Rev. B* **83**, 235427 (2011).
- <sup>19</sup>Y. Francescato, V. Giannini, and S. A. Maier, *ACS Nano* **6**, 1830 (2012).
- <sup>20</sup>Y. Sonnefraud, N. Verellen, H. Sobhani, G. A. E. Vandenbosch, V. V. Moshchalkov, P. Van Dorpe, P. Nordlander, and S. A. Maier, *ACS Nano* **4**, 1664 (2010).
- <sup>21</sup>Y. H. Fu, J. B. Zhang, Y. F. Yu, and B. Luk'yanchuk, *ACS Nano* **6**, 5130 (2012).
- <sup>22</sup>A. E. Cetin and H. Altug, *ACS Nano* **6**, 9989 (2012).
- <sup>23</sup>Y. Zhang, T. Q. Jia, H. M. Zhang, and Z. Z. Xu, *Opt. Lett.* **37**, 4919–4921 (2012).
- <sup>24</sup>J. B. Lassiter, H. Sobhani, J. A. Fan, J. Kundu, F. Capasso, P. Nordlander, and N. J. Halas, *Nano Lett.* **10**, 3184 (2010).
- <sup>25</sup>N. A. Mirin, K. Bao, and P. Nordlander, *J. Phys. Chem. A* **113**, 4028 (2009).
- <sup>26</sup>M. Hentschel, M. Saliba, R. Vogelgesang, H. Giessen, A. P. Alivisatos, and N. Liu, *Nano Lett.* **10**, 2721–2726 (2010).
- <sup>27</sup>J. A. Fan, C. Wu, K. Bao, J. Bao, R. Bardhan, N. J. Halas, V. N. Manoharan, P. Nordlander, G. Shvets, and F. Capasso, *Science* **328**, 1135 (2010).
- <sup>28</sup>A. E. Miroshnichenko and Y. S. Kivshar, *Nano Lett.* **12**, 6459–6463 (2012).
- <sup>29</sup>K. Aydin, I. Bulu, K. Guven, M. Kafesaki, C. M. Soukoulis, and E. Ozbay, *New J. Phys.* **7**, 168 (2005).
- <sup>30</sup>R. Singh, I. A. Al-Naib, Y. Yang, D. R. Chowdhury, W. Cao, C. Rockstuhl, T. Ozaki, R. Morandotti, and W. Zhang, *Appl. Phys. Lett.* **99**, 201107 (2011).
- <sup>31</sup>Y. H. Fu, A. Q. Liu, W. M. Zhu, X. M. Zhang, D. P. Tsai, J. B. Zhang, T. Mei, J. F. Tao, H. C. Guo, X. H. Zhang, J. H. Teng, N. I. Zheludev, G. Q. Lo, and D. L. Kwong, *Adv. Funct. Mater.* **21**, 3589 (2011).
- <sup>32</sup>R. Singh, I. A. Al-Naib, M. Koch, and W. Zhang, *Opt. Express* **19**, 6312 (2011).
- <sup>33</sup>I. Al-Naib, R. Singh, C. Rockstuhl, F. Lederer, S. Delprat, D. Rocheleau, M. Chaker, T. Ozaki, and R. Morandotti, *Appl. Phys. Lett.* **101**(7), 071108 (2012).
- <sup>34</sup>Y. Moritake, Y. Kanamori, and K. Hane, *Opt. Lett.* **39**, 4057 (2014).
- <sup>35</sup>Y. Moritake, Y. Kanamori, and K. Hane, *Appl. Phys. Lett.* **107**, 211108 (2015).
- <sup>36</sup>Y. Moritake, Y. Kanamori, and K. Hane, *Opt. Express* **24**, 9332 (2016).
- <sup>37</sup>D. J. Cho, F. Wang, X. Zhang, and Y. R. Shen, *Phys. Rev. B* **78**, 121101 (2008).
- <sup>38</sup>J. Wang, X. Liu, L. Li, J. He, C. Fan, Y. Tian, P. Ding, D. Chen, Q. Xue, and E. Liang, *J. Opt.* **15**, 105003 (2013).
- <sup>39</sup>F. Zhang, X. Huang, Q. Zhao, L. Chen, Y. Wang, L. Qiang, X. He, C. Li, and K. Chen, *Appl. Phys. Lett.* **105**, 172901 (2014).
- <sup>40</sup>N. Niakan, M. Askari, and A. Zakery, *J. Opt. Soc. Am. B* **29**, 2329 (2012).
- <sup>41</sup>X. R. Jin, J. Park, H. Zheng, S. Lee, Y. Lee, J. Y. Rhee, K. W. Kim, H. S. Cheong, and W. H. Jang, *Opt. Express* **19**, 21652 (2011).
- <sup>42</sup>Z.-G. Dong, H. Liu, M.-X. Xu, T. Li, S.-M. Wang, S.-N. Zhu, and X. Zhang, *Opt. Express* **18**, 18229 (2010).
- <sup>43</sup>N. E. J. Omaghali, V. Tkachenko, A. Andreone, and G. Abbate, *Sensors* **14**, 272 (2014).
- <sup>44</sup>P. B. Johnson and R. W. Christy, *Phys. Rev. B* **6**, 4370 (1972).
- <sup>45</sup>E. Prodan, C. Radloff, N. J. Halas, and P. Nordlander, *Science* **302**, 419 (2003).
- <sup>46</sup>E. E. Radescu and G. Vaman, *Phys. Rev. E* **65**, 046609 (2002).
- <sup>47</sup>T. Kaelberer, V. A. Fedotov, N. Papisimakis, D. P. Tsai, and N. I. Zheludev, *Science* **330**, 1510 (2010).
- <sup>48</sup>V. A. Fedotov, A. V. Rogacheva, V. Savinov, D. P. Tsai, and N. I. Zheludev, *Sci. Rep.* **3**, 2967 (2013).